Regional US carbon sinks from three-dimensional atmospheric CO_2 sampling

Cyril Crevoisier[a,b,1], Colm Sweeney[c,d], Manuel Gloor[e], Jorge L. Sarmiento[b], and Pieter P. Tans[d]

[a]Laboratoire de Météorologie Dynamique, Centre National de la Recherche Scientifique, Institut Pierre Simon Laplace, Ecole Polytechnique, 91128 Palaiseau Cedex, France; [b]Atmospheric and Oceanic Sciences Program, Princeton University, Princeton, NJ 08544; [c]Cooperative Institute for Research in Environmental Sciences, University of Colorado at Boulder, Boulder, CO; [d]National Oceanic and Atmospheric Administration/Earth System Research Laboratory, Boulder, CO 80305; and [e]Earth and Biosphere Institute and School of Geography, University of Leeds, Leeds, United Kingdom

Edited by Bev E. Law, Oregon State University, and accepted by the Editorial Board August 10, 2010 (received for review January 6, 2009)

Studies diverge substantially on the actual magnitude of the North American carbon budget. This is due to the lack of appropriate data and also stems from the difficulty to properly model all the details of the flux distribution and transport inside the region of interest. To sidestep these difficulties, we use here a simple budgeting approach to estimate land-atmosphere fluxes across North America by balancing the inflow and outflow of CO_2 from the troposphere. We base our study on the unique sampling strategy of atmospheric CO_2 vertical profiles over North America from the National Oceanic and Atmospheric Administration/Earth System Research Laboratory aircraft network, from which we infer the three-dimensional CO_2 distribution over the continent. We find a moderate sink of 0.5 ± 0.4 PgC y^{-1} for the period 2004–2006 for the coterminous United States, in good agreement with the forest-inventory-based estimate of the first North American State of the Carbon Cycle Report, and averaged climate conditions. We find that the highest uptake occurs in the Midwest and in the Southeast. This partitioning agrees with independent estimates of crop uptake in the Midwest, which proves to be a significant part of the US atmospheric sink, and of secondary forest regrowth in the Southeast. Provided that vertical profile measurements are continued, our study offers an independent means to link regional carbon uptake to climate drivers.

atmospheric composition | biogeochemistry | carbon cycle | greenhouse gases

Knowledge of today's carbon sources and sinks, their spatial distribution, and their variability in time is one of the essential ingredients for predicting future carbon dioxide (CO_2) atmospheric levels, and in turn the anthropogenic perturbation of radiative forcing by CO_2. Ocean uptake of anthropogenic carbon can be estimated with fairly high accuracy, implying a global net land sink of ∼1 PgC y^{-1} over the past two decades when combined with atmospheric records and fossil fuel emissions (1; see also *SI Text*). However, the location and understanding of underlying mechanisms of this land sink remain controversial. Until recently, the dominant consensus has been that a strong land sink is located in the northern hemisphere midlatitudes, although attempts (2–9) to partition the sink further between Eurasia and North America have yielded diverse values ranging from 0.4 to 1.4 PgC y^{-1} for the temperate North American sink, with associated formal uncertainties ranging from 0.4 to 0.8 PgC y^{-1} (Table 1). This large spread in the estimates comes partially from temporal variability of the sink, but also stems from the lack of appropriate observations, which strongly impacts "top-down" atmospheric approaches.

The traditional top-down approach exploits, in essence, the accumulation or depletion of CO_2 in the overlying air as a constraint on carbon sources and sinks at the surface. It uses atmospheric transport models in an inverse mode to determine the spatiotemporal land-air surface flux distribution that gives the best match to a set of atmospheric CO_2 data. Strong biases in the estimates may arise from (*i*) the specific nature of surface fluxes originating from a strong diurnal and seasonal cycle in land vegetation; (*ii*) limitations in state-of-the-art atmospheric transport models, particularly in terms of near-surface to midtroposphere air exchange, with the choice of the transport model used in the estimation critically influencing the results (10–12); and (*iii*) limitations in atmospheric CO_2 sampling (4, 5, 13). In particular, atmospheric concentration measurements have been predominantly made at remote locations to avoid the vicinity of large point sources or rapidly varying fluxes such as those due to photosynthesis and respiration on land, and fossil fuel emissions. Point source flux signals are thus strongly diluted. Also, being mostly made at the surface, the measurements also lack information in the vertical dimension that is not only necessary to characterize the surface fluxes but also essential to validate and calibrate model transport. Given that the spread in the flux estimates obtained with the traditional atmospheric inverse approach comes largely from the difficulty in modeling properly all the details of the flux distribution and transport inside the region of interest, a reasonable alternative approach would be to not try to model that detail at all, but to just look at the inflow and outflow at the boundaries of this region.

To that end, we leverage a unique vertical profile sampling strategy that was implemented by National Oceanic and Atmospheric Administration/Earth System Research Laboratory (NOAA/ESRL) to extract signatures of the exchange of CO_2 and other trace gases over the continent and their associated variability, and to constrain representations of atmospheric mixing in chemical transport models. The use of such data in a data assimilation system or in a traditional atmospheric approach may result in a powerful constraint on carbon budgets, even when using weaker or no a priori constraints on fluxes (8). However, this would involve solving the problem of the design of an appropriate error covariance structure that would be assigned to vertical transport models. In this paper, we focus on a particular strength of these data, which is the opportunity they provide to design a method avoiding the need for detailed modeling of fluxes and transport processes to estimate the North American temperate sink. Here, we use the vertical profile sampling strategy to estimate the full three-dimensional tropospheric CO_2 distribution over North America and use analyzed winds to study mass exchange pathways over the continent. Relying on a simple budgeting approach and the assumption that large-scale temporal and spatial variability dominate the change in the three-dimensional CO_2 distribution, we derive a previously undescribed

Author contributions: M.G. and P.P.T. designed research; C.C. performed research; C.S. contributed data; C.C., M.G., J.L.S., and P.P.T. interpreted results; C.C. and C.S. analyzed data; and C.C. wrote the paper.

The authors declare no conflict of interest.

This article is a PNAS Direct Submission. B.E.L. is a guest editor invited by the Editorial Board.

Freely available online through the PNAS open access option.

[1]To whom correspondence should be addressed. E-mail: cyril.crevoisier@lmd.polytechnique.fr.

This article contains supporting information online at www.pnas.org/lookup/suppl/doi:10.1073/pnas.0900062107/-/DCSupplemental.

Downloaded at Palestinian Territory, occupied on December 25, 2021

www.manaraa.com

Table 1. Estimates of North American (NA) atmospheric carbon sinks (in $PgC\,y^{-1}$)

	1980–1989	1988–1992	1992–1996				2001–2006	2004–2006
Temperate NA sink	−0.71 to −0.37*,† (2)	−1.2 ± 0.4 (3)	−0.81 ± 0.72 (4)	−0.89 ± 0.39 (5)	−1.26 ± 0.23 (6)	−0.93 ± 0.71 (7)	−0.575 with 95% confidence that estimate is within 50% (9)*	−0.51 ± 0.41 This study†
Method	Land based	Atmospheric inversion	Atmospheric inversion	Atmospheric inversion	Atmospheric inversion	Joint ocean/ atm. inversion	Land based	
El Niño Southern Oscillation index	High	Neutral	Moderate				Neutral	Neutral
North Atlantic Oscillation index	Neutral	High	High				Neutral	Neutral
Volcanic eruptions	El Chichón	Pinatubo	Aftermath of Pinatubo					–

*Land-based estimate, corrected to account for fluxes to the atmosphere released in another region.
†Estimate in the coterminous United States.

estimate of the North American sink with results at a regional level that we compare with previously published estimates.

A Three-Dimensional CO_2 Distribution

The data consist of regular aircraft-based measurements of vertical CO_2 profiles up to a height of 8 km performed by NOAA/ESRL as part of the North American Carbon Program (14) at 20 locations (Table S1) covering most of North America, including Hawaii, once to twice a month, for the three-year period 2004–2006. Most measurements were performed around noon, which is the time most representative of the daily average CO_2 column (10). All together, about 25,000 measurements covering the three-year period are used in this study.

Analysis of the profiles reveals strong signatures of CO_2 exchanges over the continent (Fig. 1). During summer in the Northern Hemisphere, the atmospheric CO_2 mole fraction is lower in the boundary layer (BL) than in the free troposphere (FT), reflecting the impact of vegetation uptake, which exceeds vegetation respiration and fossil fuel emissions. The situation is reversed in winter, when respiration and fossil fuel emissions

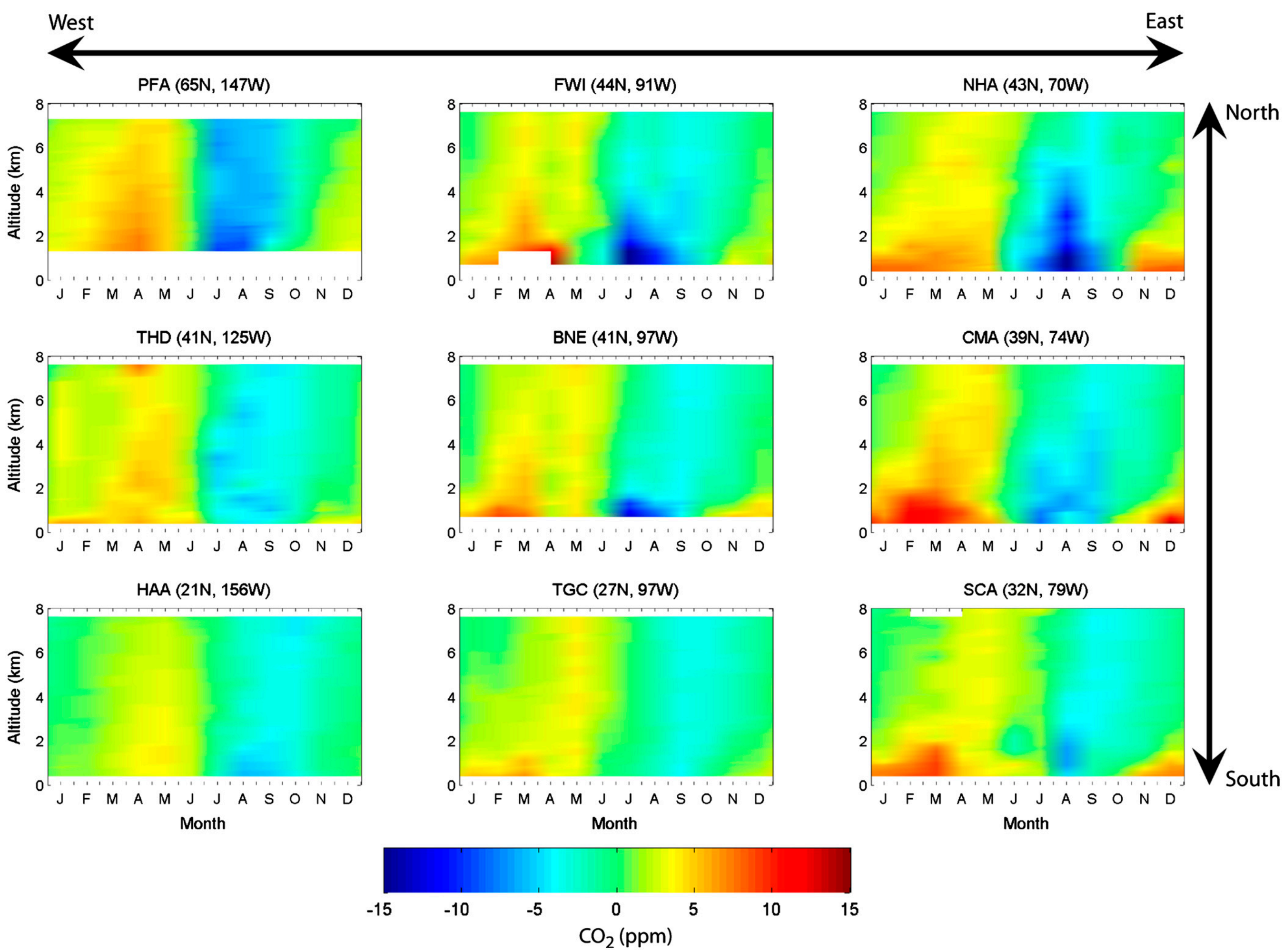

Fig. 1. Altitude-time CO_2 plots for nine sites of the NOAA/ESRL network as derived from measurements from which the deseasonalized smoothed trend at Mauna Loa Observatory is removed. The plots are arranged according to the geographical location of the stations.

ENVIRONMENTAL SCIENCES

Downloaded at Palestinian Territory, occupied on December 25, 2021
www.manaraa.com

become dominant. The farther to the North, the more pronounced the CO_2 seasonal cycle and the BL-FT gradient (Fig. 1 and Fig. S1), following the vegetation distribution. The difference between BL and FT CO_2 mole fraction is larger in the East than in the West (Fig. 1 and Fig. S1), due to strong West to East transport, which enhances the concentration difference as air masses are transported across the country, and because BL-FT exchange is too slow to effectively erase the difference.

Building on the clear qualitative coherence of the spatial patterns in the data (Fig. 1), we first interpolate the profiles using a Kriging geostatistical interpolation method (15) to obtain the 2D distribution of CO_2 at multiple altitudes over the surface for a single climatological year across North America, up to 55 °N (Fig. 2). This northern limit is dictated by the location of the stations, which cover only the coterminous United States and southern Canada. The Southwest of the United States is not covered by the current aircraft network; hence the variability of CO_2 in this region is not as well defined by the data as the rest of North America. However, (*i*) no significant carbon source or sink is expected to be located in the Southwest region (8) and (*ii*) variability in air propagating from the Asian continent will be considerably attenuated when entering the North American troposphere. This is because CO_2 profiles over the oceans are less variable compared to continental profiles, because the air has recently been exposed only to air-sea fluxes. These fluxes vary much less than air-land fluxes, because they are moderated by comparatively slower air-sea gas exchange, with an equilibration time of about one year (16).

Incoming and Outgoing CO_2 Pathways

Following the actual coverage of the aircraft network, we focus our study on a tropospheric control volume over North America (Fig. S2). Analyzed wind fields give us a means to estimate the incoming and outgoing CO_2 transports that determine the mole fraction differences illustrated in Figs. 1 and 2. We compute carbon transport fluxes due to horizontal advection using the interpolated three-dimensional CO_2 distribution and National Centers for Environmental Prediction (NCEP) analyzed winds for the three-year period 2004–2006 (see the *Materials and Methods* section). The annual mean of carbon transport fluxes due to horizontal advection across the edges of the control volume and between various regions within this volume is plotted in Fig. 3. On average, a strong West to East transport is observed, coming from both the three-dimensional wind distribution and the location of sources and sinks at the surface.

High horizontal outgoing transport fluxes are found along the East Coast, due to the eastward winds and to the elevated CO_2 source due to fossil fuel emissions from Texas northward along the East Coast. On a monthly scale (Fig. S3), these high outgoing transport fluxes are mainly found during winter (when fossil fuel emissions are stronger and land uptake is minimal), with a maximum in January and February. They then decrease through spring to fall due to the growing vegetation in the East and Midwest. The summertime absolute values of the horizontal transport fluxes are small, however, highlighting the fact that the land vegetation carbon sink only slightly overcomes the fossil fuel emissions. On the West Coast, the horizontal CO_2 transport

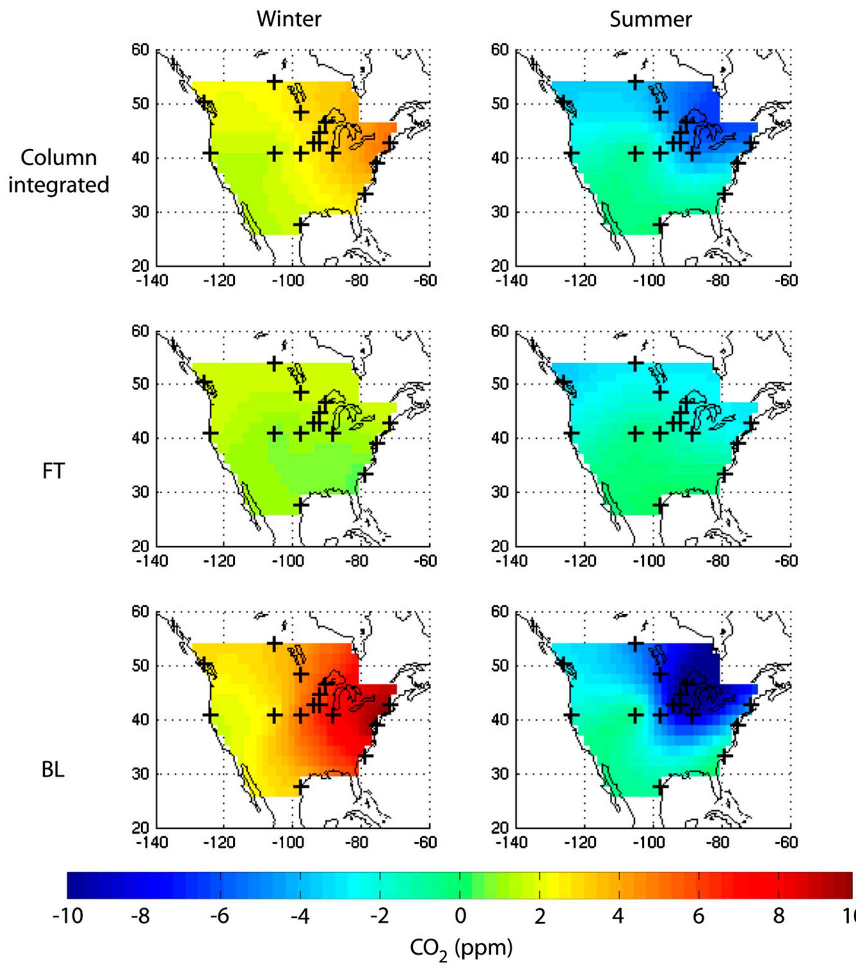

Fig. 2. Interpolated CO_2 distribution anomaly relative to the deseasonalized and smoothed trend at Mauna Loa (ppm) in winter (average from December to February) and summer (average from June to August) in the BL, FT, and integrated over the 0- to 8-km atmospheric column. Black crosses indicate the location of the 19 stations used for the Kriging interpolation.

PNAS PNAS PNAS PNAS
Downloaded at Palestinian Territory, occupied on December 25, 2021
www.manaraa.com

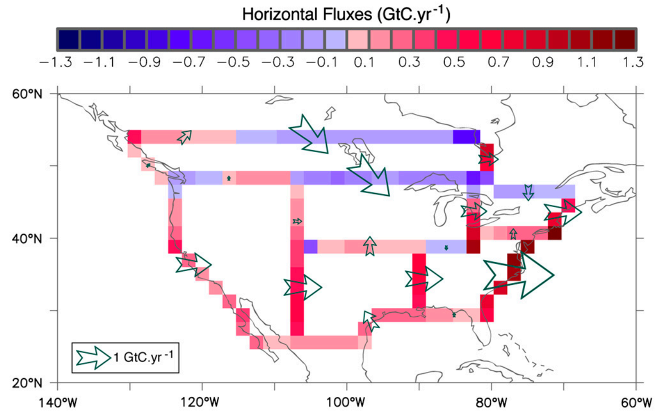

Fig. 3. Annual mean of horizontal advective fluxes of CO_2 in $PgC\,y^{-1}$. Positive values indicate northward and/or eastward flows. The area of the arrows shows the absolute value of the fluxes going in or out of each region. The arrow angles indicate the direction of mean circulation. Region boundaries have been chosen according to station location (Fig. 2), state boundaries, and vegetation distribution (Fig. 4).

fluxes are smaller and exhibit a less pronounced seasonal cycle, following the low temporal variability of CO_2 in this region, which is mostly influenced by the well-mixed and slowly varying troposphere due to transport over the Pacific Ocean. The change of sign found at the northern border of the measurement space (outgoing flux in the West and incoming flux in the central region) comes from the shift in the wind direction from northward in the West to southward in the center and East, acting on the seasonal cycle of Canadian forest uptake and release of CO_2 north of the control volume. Finally, the horizontal transport fluxes found at the southern border are generally small, due to the canceling effect of seasonal changes in the inflow and outflow through the southern edge of the volume (Fig. S3). On average, in the South, CO_2 tends to enter the control volume from the Gulf of Mexico.

The availability of CO_2 profiles up to a height of 8 km provides an opportunity to analyze at which vertical level of the atmosphere CO_2 enters or leaves the North American troposphere. We compute the horizontal advective transports separately for the BL and the FT. As suggested by the relative magnitudes of the horizontal gradients in the BL and FT shown in Figs. 1 and 2, most of the transport on the East Coast (about 80% on average) happens in the BL, especially in winter and summer when strong surface fluxes prevail. In contrast, across the West Coast only 65% of CO_2 is horizontally transported in the BL, revealing the need for measurements at high altitude to fully capture the whole flow of CO_2 entering the control volume. This East-West difference stems partly from the relatively small variations in CO_2 profiles coming from the oceanic regions and measured along the West Coast, with a reduced BL-FT gradient (Figs. 1 and 2). CO_2 enters across the northern border mostly in the BL, but the signal is more diluted along the first kilometers above the surface than in the East, as suggested by Fig. 1. On the East and North borders, where a strong seasonal cycle is observed at the surface, a peculiar behavior of the BL vs. FT flow can be observed in June and November; although during the rest of the year, both transport fluxes are of the same sign, the BL and FT transport fluxes observed during these two months are of opposite signs. This is due to the strong decrease (increase) of CO_2 in June (November), which is mostly confined to the BL and has not yet fully reached the FT.

Continental and Regional Mean Surface Fluxes

We use what we call a Direct Carbon Budgeting Approach (15) to compute surface fluxes from the interpolated CO_2 fields. For the control volume over North America defined previously (Fig. S2), we balance carbon air mass (C) flows into and out of the volume (at the surface, across the vertical edges of the volume, and at its top) and solve for the surface fluxes, according to

$$F_{\text{surf}}(x,y,t) = dC/dt(x,y,t)\text{-}F_{\text{side}}(x,y,t)\text{-}F_{\text{top}}(x,y,t). \qquad [1]$$

Details on the computation of each term are given in *Materials and Methods*. Our approach may be seen as a first attempt to exploit the availability of the profiles of CO_2 extending through most of the troposphere, which gives the opportunity to take advantage of large-scale features of atmospheric transport. This method has the advantage of relying mostly on the interpolated CO_2 data and on the reanalyzed wind distributions used to compute the advective transport fluxes $F_{\text{side}}(x,y,t)$ and thus does not rely on model representation of processes not resolved on the model grid like vertical transport (e.g., due to convection, thunderstorms, fronts and squall lines, or boundary layer dynamics), with the exception of the small convective outflow at the top (8 km) of the control volume (see below). It also strongly reduces the bias due to so-called daily and seasonal "rectification" (17). Although strong ventilation and deeper mixing of CO_2-depleted air occurring during the day and the growing season may occasionally extend to higher altitudes than 8 km (top height of aircraft profiles), measurements are usually taken in fair weather conditions when strong ventilation events are rare and the mixing should be limited to lower altitudes. It should be noted that the bias resulting from the sampling in fair weather is likely to be small (see *SI Text*). Finally, by focusing on a limited volume of the troposphere, biases in remote regions such as the Tropics do not affect our estimates.

In the absence of independent observations, uncertainties of the method have been examined based on its application to fields of simulated CO_2 mole fraction with state of the art atmospheric transport models and a range of surface flux fields (15; see also *SI Text*). Formal uncertainties of the Kriging approach, which account for the errors introduced by the interpolation of the data, have also been evaluated using model simulations and measurements (15; see also *SI Text*). Here, we apply the method to real data.

From the variation of carbon in the volume and the advective fluxes, we find a surface flux of CO_2 into the whole North American volume of 1.22 ± 0.41 $PgC\,y^{-1}$. Given estimated fossil fuel emissions for the same period of 1.73 ± 0.04 $PgC\,y^{-1}$ (18), we estimate a terrestrial carbon sink in coterminous North America (up to 55 °N) of 0.5 ± 0.4 $PgC\,y^{-1}$ for the period January 2004–December 2006. This value does not include the net outflow of CO_2 at 8 km due to convection, which is not estimated from the data. Simulations performed by various models yield an additional convective outflow of 0.1 $PgC\,y^{-1}$ there (15), giving a surface sink under the volume of 0.6 $PgC\,y^{-1}$.

By dividing the control volume into various regions (Fig. 4), we find that the land carbon sinks are mainly located in three regions: Midwest states (52%), which are characterized by extensive agriculture; the southeastern regions (22%), where most of the deciduous forests are located; and the southern part of the boreal region (18%). The western and southern regions appear to be neutral. For the coterminous United States, including a small part of southern Quebec and Ontario (Fig. 4), the sink is estimated as 0.5 $PgC\,y^{-1}$.

Our estimates agree well with forest-inventory-based estimates of the State of the Carbon Cycle Report (SOCCR) (9), which found an atmospheric sink of 0.575 $PgC\,y^{-1}$ in the United States, with half of the sink due to forest regrowth in the East (20). Given the uncertainties of each estimate, a comparison of the mean values of regional estimates should be done with caution. However, the general locations of the sinks found in our study are in good agreement with the ones reported in the SOCCR, as well as those suggested from MODIS (Moderate Resolution Imaging Spectroradiometer) satellite data combined with ecosystem modeling (21).

ENVIRONMENTAL SCIENCES

Downloaded at Palestinian Territory, occupied on December 25, 2021

www.manaraa.com

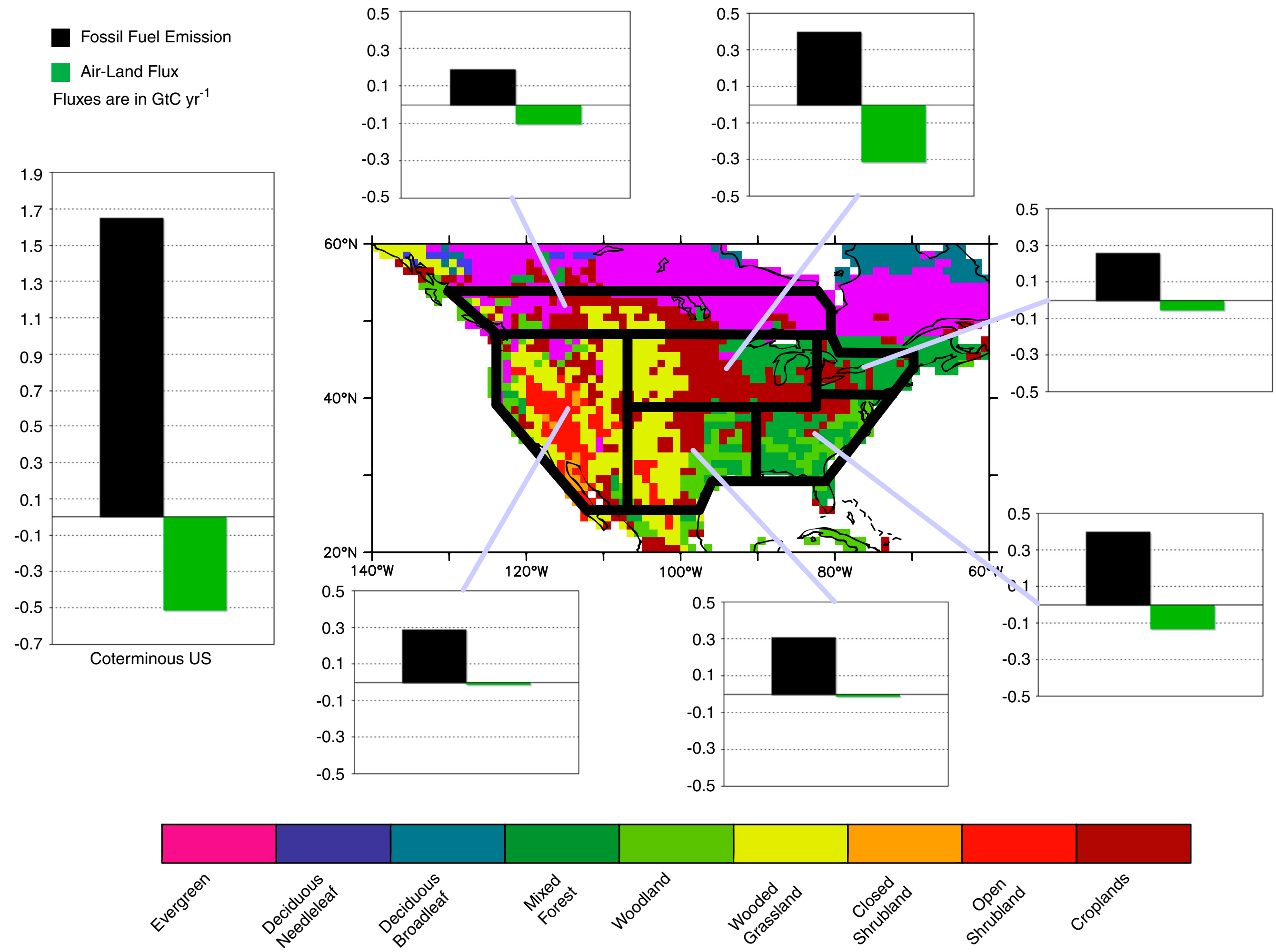

Fig. 4. Vegetation map (19) and estimates of fossil fuel emissions and air-land fluxes in North America. Air-land fluxes are computed by the difference between the surface fluxes estimated by our direct carbon budgeting approach and estimates of fossil fuel emissions (18).

Discussion

The strong atmospheric sink in the agricultural region is consistent with the difference in the spatial distribution of agricultural production and product consumption: a strong atmospheric uptake by crops during the growing season in the Midwest states, while much of the release of carbon associated with consumption of agricultural products occurs in other regions, in the United States and abroad. It must thus be pointed out that this apparent atmospheric sink in the Midwest does not imply a long-term carbon sequestration (22). In particular, strong release of carbon associated with agricultural consumption occurs in the pastureland in the southern and western regions, which, in addition to sparse vegetation (desert), might explain the low fluxes we find in these regions. However, due to the very low information content of the current network in that region, this result should be treated with caution. Based on cropland production (23) and on cropland area (24), carbon uptake by crops in the Midwest has been estimated to be 0.25 $PgC\,y^{-1}$, which is of the order of our Midwest sink estimate (0.31 $PgC\,y^{-1}$). Our estimate also includes uptake of carbon by regrowing forest near the Great Lakes. The sink we find in the Southeast and, to a lesser extent, in the Northeast is consistent with forest regrowth exceeding harvest (20, 25, 26) (Fig. S4) and with favorable climate conditions in the Southeast where, as opposed to the Northeast, precipitation has been increasing over the last decade (Fig. S5).

As compared to previous estimates (Table 1), ours is similar to inventory-based estimates for the 1980–1989 decade (2), but smaller than estimates based on an analysis of annual mean mole fractions using atmospheric transport inversions for the periods 1989–1992 (3) and 1992–1996 (4–7). These periods have much different global atmosphere-land fluxes consistent with different external controls and land-atmosphere fluxes in the aftermath of the Mount Pinatubo eruption. Therefore, before the response of carbon storage on land to anomalous climate events and land management are fully understood, comparisons are difficult to make. Nonetheless, with regard to external controls for the period 2004–2006, climate fields are fairly average compared to the 1990–2006 period except that the temperature is higher by about 1 K (Fig. S5). Accordingly, thermal time (27), a proxy for growing season length, is somewhat longer than usual (Fig. S6). Increased temperatures have been shown to coincide with small but significant decreases in crop yields and thus are likely to oppose any fertilization effect of increased CO_2 levels (28). Moreover, this period is not in the aftermath of a major volcanic eruption. It is therefore reasonable to view the 2004–2006 period as having no extreme events and to assume that the fluxes and causes discussed above are characteristic of an average year with regard to climate forcing, regardless of potential local anomalies. The good agreement between our top-down estimates and previous bottom-up estimates, as well as the reasonable behavior with respect to climate, give some confidence in the results and suggest that it would be highly desirable to further exploit the aircraft profiling method.

Although we consider our estimates as likely being representative of average conditions, only continuation and increase in frequency of the measurements will make it possible to follow

Downloaded at Palestinian Territory, occupied on December 25, 2021
www.manaraa.com

the evolution of the North American sink. Moreover, the availability of multiple profile sampling of CO_2, combined here with our direct carbon budgeting approach, provides a means to partition the sink in different regions and to thus link variations in carbon uptake to vegetation, climate and human drivers, a well-defined priority of the North American Carbon Program (NACP). Given the promise of the simple mass balance method and given the particular strength of using multiple profile measurements as opposed to only surface measurements in an atmospheric inversion (8), we would recommend expanding the coverage of appropriate observations with (*i*) more observations at all sites to allow us to detect interannual variability and (*ii*) an increase in site locations both in the coterminous United States and in other terrestrial regions where the method can work and the carbon budget is poorly understood, namely the Amazon basin or, more generally, the tropical region, although this would require a better understanding of the convective outflow across the 8-km level because these regions have much stronger and deeper convection compared to midlatitudes. In our view, the initial results presented here demonstrate a feasible strategy for constraining the large-scale carbon budgets of these regions.

Materials and Methods

We interpolate the profiles using a Kriging technique (29). We take into account the spatial continuity of the CO_2 field using modeled spatial covariance (15). The subgrid variability is taken from ref. 30. We estimate the horizontal CO_2-carbon advective transport fluxes across the edges of the control volume V shown in Fig. S2 from

$$F_{\text{horizontal}} = -\iint_S \rho\chi \boldsymbol{u}\cdot \boldsymbol{n} dS,$$

where χ is the CO_2 dry air mole fraction, ρ is air density, $\boldsymbol{u}$ is the 3D-wind field, S is the surface vertically bounding V (extending from the surface to 8 km), and $\boldsymbol{n}$ is the normal to S. Here, χ is the interpolated CO_2 profile anomaly relative to Mauna Loa. The wind distribution $\boldsymbol{u}$ used in our study and shown in Fig. S2 is taken from the NCEP (31) reanalysis. Nearly identical results have been obtained with the European Centre for Medium-Range Weather Forecasts wind distribution (32).

We estimate the surface fluxes using the volume-integrated continuity equation, which gives the carbon budget in the control volume V shown in Fig. S2,

$$\left.\frac{\partial C}{\partial t}\right|_V = \frac{\partial}{\partial t}\iiint_V \rho\chi dV = -\iint_S \rho\chi \boldsymbol{u}.\boldsymbol{n} dS + F_{\text{vertical}} + F_{\text{surf}},$$

where C is the CO_2-carbon mass content inside V, S is the surface enveloping V (including the top at 8 km and the bottom, with a surface wind velocity equal to zero), t is time, F_{vertical} is the carbon flux, other than vertical advection, at the top of V, and F_{surf} is the carbon surface flux. Terms of the equation represent (*i*) the change of carbon inside V; (*ii*) carbon fluxes due to advection; (*iii*) vertical carbon fluxes, other than vertical advection, between V and the upper atmosphere, at 8 km; and (*iv*) carbon exchanges between V and the ground, which are the sum of natural vegetation, fossil fuel emissions, and nonvegetation fluxes such as CO_2 stored in reservoirs and going into rivers.

All the measurements were made by the NOAA/ESRL Aircraft Project using automated portable flask packages. A separate portable compressor package is used to flush the air samples through a 0.7-L borosilicate glass flask at 10–18 L/min. Measurement was done by first cryogenically drying the sample gas and measuring the mole fraction using a nondispersive infrared analyzer and three World Meteorological Organization CO_2 reference standards. Samples are collected at weekly to monthly intervals from 500 m above ground to 8 km and analyzed at NOAA/ESRL within a week of collection. Aircraft are equipped with single air inlets extending more than 6 in. off the fuselage to avoid contamination from aircraft emissions. Simultaneous measurements of a variety of halocarbons and CO provide an independent indication of cabin air or engine exhaust contamination.

ACKNOWLEDGMENTS. This research was funded by the Cooperative Institute for Climate Science under award NA17RJ2612 from the National Oceanic and Atmospheric Administration, U.S. Department of Commerce, by the Carbon Mitigation Initiative, with support provided by the Ford Motor Company, and by the U.S. Department of Energy's Office of Science (BER) through the Northeastern Regional Center of the National Institute for Climatic Change Research. The statements, findings, conclusions, and recommendations are those of the authors and do not necessarily reflect the views of the National Oceanic and Atmospheric Administration, or the U.S. Department of Commerce.

1. Sabine CL, et al. (2004) The oceanic sink for anthropogenic CO_2. *Science* 305:367–371.
2. Pacala SW, et al. (2001) Consistent land- and atmosphere-based U.S. carbon sink estimates. *Science* 292:2316–2320.
3. Fan S-M, Sarmiento JL, Gloor M, Pacala SW (1999) On the use of regularization techniques in the inverse modeling of atmospheric carbon dioxide. *J Geophys Res* 104:21503–21512.
4. Gurney KR, et al. (2002) Towards robust estimates of CO_2 sources and sinks using atmospheric transport models. *Nature* 415:626–630.
5. Gurney KR, et al. (2004) Transcom 3 inversion intercomparison: Model mean results for the estimation of seasonal carbon sources and sinks. *Global Biogeochem Cycles* 18:GB1010.
6. Baker DF, et al. (2006) Transcom 3 inversion intercomparison: Impact of transport model errors on the interannual variability of regional CO_2 fluxes, 1988–2003. *Global Biogeochem Cycles* 20:GB1002.
7. Jacobson AR, Mikaloff Fletcher SE, Gruber N, Sarmiento JL, Gloor M (2007) A joint atmosphere-ocean inversion for surface fluxes of carbon dioxide: 1. Methods and global-scale fluxes. *Global Biogeochem Cycles* 21:GB1019.
8. Peters W, et al. (2007) An atmospheric perspective on North American carbon dioxide exchange: CarbonTracker. *Proc Natl Acad Sci USA* 104:18925–18930.
9. Pacala SW, et al. (2007) *The First State of the Carbon Cycle Report (SOCCR)*, eds AW King et al. (U.S. Climate Change Science Program, Washington, DC), pp 69–91.
10. Stephens BB, et al. (2007) Weak northern and strong tropical land carbon uptake from vertical profiles of atmospheric CO_2. *Science* 316:1732–1735.
11. Yang Z, et al. (2007) New constraints on Northern Hemisphere growing season net flux. *Geophys Res Lett* 34:L12807.
12. Prather MJ, Zhu X, Strahan SE, Steenrod SD, Rodriguez JM (2008) Quantifying errors in trace species transport modeling. *Proc Natl Acad Sci USA* 105:19617–19621.
13. Gloor M, et al. (2001) What is the concentration footprint of a tall tower? *J Geophys Res* 106:17831–17840.
14. North American Carbon Program Implementation Strategy Group (2005) Science Implementation Strategy for the North American Carbon Program, http://www.isse.ucar.edu/nacp/.
15. Crevoisier C, et al. (2006) A direct carbon budgeting approach to infer carbon sources and sinks. Design and synthetic application to complement the NACP observation network. *Tellus* 58B:366–375.
16. Lynch-Stieglitz J, Stocker TF, Broecker WS, Fairbanks RG (1995) The influence of air-sea exchange on the isotopic composition of oceanic carbon: Observations and modeling. *Global Biogeochem Cycles* 9:653–665.
17. Denning AS, Fung IY, Randall AD (1995) Latitudinal gradient of atmospheric CO_2 due to seasonal exchange with land biota. *Nature* 376:240–243.
18. Marland G, Boden T, Andres RJ (2007) National CO_2 emissions from fossil-fuel burning, cement manufacture, and gas flaring. http://cdiac.ornl.gov/trends/emis_mon/stateemis/emis_state.html.
19. Hansen M, DeFries R, Townshend JRG, Sohlberg R (1998) UMD Global Land Cover Classification, 1 Kilometer, 1.0, Department of Geography, University of Maryland, College Park, Maryland, 1981–1994.
20. Houghton RA, Hackler JL (2000) Changes in terrestrial carbon storage in the United States 1. The roles of agriculture and forestry. *Global Ecol Biogeogr* 9:125–144.
21. Potter C, Klooster S, Huete A, Genovese V (2007) Terrestrial carbon sinks for the united states predicted from MODIS satellite data and ecosystem modeling. *Earth Interact* 11:1–21.
22. Verma SB, et al. (2005) Annual carbon dioxide exchange in irrigated and rainfed maize-based agroecosystems. *Agr Forest Meteorol* 131:77–96.
23. United States Department of Agriculture (2006) *Crop Production 2006 Summary* (National Agricultural Statistics Service report).
24. Waisanen PJ, Bliss NB (2002) Changes in population and agricultural land in conterminous United States countries. *Global Biogeochem Cycles* 16:1137.
25. Hurtt GC, et al. (2002) Projecting the future of the U.S. carbon sink. *Proc Natl Acad Sci USA* 99:1389–1394.
26. Hurtt GC, et al. (2006) The underpinnings of land-use history: Three centuries of global gridded land-use transitions, wood harvest activity, and resulting secondary lands. *Glob Change Biol* 12:1208–1229.
27. Masle J, Doussinault G, Farquhar GD, Sun B (1989) Foliar stage in wheat correlates better to photothermal time than to thermal time. *Plant Cell Environ* 12:235–247.
28. Lobell DB, Field CW (2007) Global scale climate-crop yield relationships and the impacts of recent warming. *Environ Res Lett* 2:014002.
29. Matheron G (1965) *Regionalized Variables and Their Estimation (Les Variables régionalisées et leur estimation)* (Masson, Paris) p 306.
30. Lin JC, et al. (2004) An empirical analysis of the spatial variability of atmospheric CO_2: Implications for inverse analyses and space-borne sensors. *Geophys Res Lett* 31:L23104.
31. Kalnay E, et al. The NCEP/NCAR 40-year reanalysis project. *Bull Am Meteorol Soc* 77:437–470.
32. Uppala SM, et al. (2005) The ERA-40 re-analysis. *Quart J Roy Meteorol Soc* 131:2961–3012.

ENVIRONMENTAL SCIENCES
Downloaded at Palestinian Territory, occupied on December 25, 2021
www.manaraa.com